JOURNAL OF MATERIALS SCIENCE 30 (1995) 3652–3657

Hardening of 316L stainless steel by laser surface alloying

F. LAROUDIE, C. TASSIN, M. PONS
Laboratoire Science des Surfaces et Matériaux Carbonés, URA CNRS n° 413, ENS d'Electrochimie et d'Electrométallurgie de Grenoble, Institut National Polytechnique de Grenoble, BP 75 Domaine Universitaire, F-38402 Saint-Martin d'Hères, France

The goal of this study is to investigate different hardening routes for 316L stainless steel by laser surface alloying. We have investigated the formation of iron–chromium carbides by SiC or carbon incorporation, the alloying with submicronic particles of TiC and the precipitation of titanium carbide from mixtures of Ti and SiC. For each hardening route we present the microstructures and the hardness of the processed surface alloys and the conditions leading to the best compromise between highest hardness, best homogeneity and lowest occurrence of cracks. From these results it can be reasoned that hardening by iron–chromium carbides is the best hardening route and that this surface alloy might be a good candidate for tribological applications.

1. Introduction

The more traditional way for improving or altering the surface properties of solids involves the deposition of films and coatings from solid, liquid and vapour sources [1]. A more recent approach is based on the modification of existing surfaces using directed energy sources such as laser beams [2]. The laser process parameters can easily be adjusted to obtain the desired surface alloy composition and microstructure, thus improving the fatigue, wear, or corrosion resistance of the bulk material.

We focus this study on laser-surface alloying of 316L stainless steel. This process consists of melting the surface of the base alloy with known amounts of other materials, mixing these components and allowing them to solidify rapidly. This process leads to a surface layer with a chemical composition and properties which are different from those of the substrate material. The range of attainable surface modifications is enlarged by the possibility of introducing different elements. This process is usually classified into either preplaced powder alloying [3] or blown powder alloying [4–6]. The former method was used for this study.

The 316L austenitic stainless steel substrate is widely used owing to its high corrosion resistance, but, due to its low hardness (200 H_V), its tribological properties are very poor [7]. Moreover, because of its austenitic structure, it cannot be hardened by heat treatment and therefore there is no easy means for improving its wear resistance [8].

AISI 304 stainless steel was hardened by laser melt injection of 140–70 mesh TiC particles. The microhardness of the austenitic matrix increased from 150 H_V to values of about 200–250 H_V [9]. Laser alloying of a 12% Cr stainless steel with Cr_3C_2 powder was also carried out. The surface-alloyed region exhibited a microhardness of about 1100 H_V due to the dispersion and precipitation of chromium carbides in addition to the martensitic structure [10]. Other authors studied the laser alloying of stainless steels with boron [11] and carbon [12]. In both cases, an increase in hardness versus the quantities of boron and carbon incorporated was evidenced. Rieker *et al.* [13] improved the abrasive wear resistance of a ferritic stainless steel by laser alloying with molybdenum and boron. Laser alloying of 304 stainless steel, with molybdenum alone led to an increase in hardness from 200 to 400 H_V for a surface alloy containing 10 wt % of molybdenum [14].

We present here different hardening routes for the 316L austenitic stainless steel using laser alloying, (i) formation of iron–chromium carbides by SiC or carbon incorporation, (ii) incorporation of submicronic particles of TiC, (iii) precipitation of titanium carbide.

2. Experimental procedure

The substrate material used for all the experiments was the austenitic stainless steel 316L; its composition is given in Table I. The samples, about 5 mm thick, were mechanically polished before laser irradiation. The different powders, TiC, Ti + SiC, SiC and C were deposited onto the surface by different techniques. For TiC, submicronic particles and polyethylene glycol (PEG, MW 400) were used to obtain a pasty mixture. The paste was applied onto the surface of a stainless steel block by brushing. For Ti + SiC and SiC the technique was the same, but the grain size of the powders was about 40 μm. For carbon, the powder (grain size of about 5 μm) was mixed with ethanol and sprayed onto the surface.

0022–2461

Surface alloying was carried out using a 300 W continuous wave Nd-YAG laser with argon as a shielding gas to prevent alloys from oxidizing. The beam was guided by an optical fibre to give a circular spot of 950 μm in diameter leading to a maximum power density of 4.10^8 W m^{-2}.

The samples were moved under the stationary beam using a numerically controlled X–Y table. The scanning rate is adjustable from 0 to 10 cm s^{-1} allowing control of the interaction time, $t(t = d/v$; d is beam diameter and v is scanning speed). In a few cases, such as improving tribological properties, it is not always necessary to treat the entire sample surface [4]. But in most cases (corrosion resistance, surface hardening), a complete surface alloying is required. In this study, multiple laser tracks were used and the shift between two successive tracks was kept constant. The optimum shift used to ensure a constant thickness coating was about 30% of the beam diameter ($\sim$300 μm).

The parameters which varied were the laser power P, the substrate scanning speed beneath the beam, v, and the amount of predeposited powder (surface coverage denoted s.c.). Working conditions were laid down after some preliminary experiments in which the conditions tried out were: the power of the laser between 150 and 300 W, the scanning speed between 0.1 and 3 cm s^{-1} and the amount of predeposited powder between 2 and 15 mg cm^{-2}. The criteria for determining the quality of the coatings were a compromise between highest hardness, best homogeneity and lowest occurrence of cracks. On the basis of these criteria, the best processing conditions for the various systems are listed in Table II.

The microstructure and the composition of the coatings were studied on polished cross-sections by optical and scanning electron microscopy (SEM), electron probe microanalysis (EPMA), and X-ray diffraction (XRD). The microhardness measurements were performed with a Vickers indentor at a load of 100 g on polished cross-sections over dimensions larger than one track to study the homogeneity of the coating.

TABLE I Chemical composition (wt %) of the 316L stainless steel

C	Cr	Ni	Mo	Mn	P	S	Si
≤ 0.03	17	12	2.3	2	0.04	0.03	0.75

3. Results and discussion

3.1. Hardening by formation of iron-chromium carbides

3.1.1. SiC alloying

For the incorporation of SiC in 316L stainless steel, we have selected a series of surface coverages mentioned in Table II.

3.1.1.1. Surface coverage: 5.5 mg cm^{-2} (sample 1a). XRD analysis showed that the surface alloy is composed of austenite (γ) and M_7C_3 carbides (M = Fe, Cr). It is thought that the high temperatures (greater than 3000 °C) reached during the treatment lead to the decomposition of SiC in silicon and carbon. During the solidification, silicon, and maybe some amounts of carbon dissolve in austenite, the remaining carbon leading to carbide precipitation.

A micrograph of the laser-alloyed region (about 150 μm thick) is presented in Fig. 1a. The structure is homogeneous throughout the alloy, consisting of primary austenite cells or dendrites surrounded by a fine eutectic containing M_7C_3 carbides. Nevertheless, an increase in the size of austenite cells may be observed in the heat affected zone of each track as schematized in Fig. 1b.

Microhardness measurements revealed a mean value of 500–600 H_V in the melted regions whereas the heat affected zones exhibit a lower hardness: about 450 H_V.

With the process parameters used (reported in Table II), the surface alloy is crack-free.

3.1.1.2. Surface coverage 6.5 mg cm^{-2} (sample 1b). XRD analysis showed that the surface alloy is composed of austenite and M_7C_3 carbides (M = Fe, Cr). Peaks corresponding to another phase were also detected but not identified yet. As previously, we can conclude that SiC decomposes.

A micrograph of a transversal cross-section of the alloyed region (about 150 μm thick) is illustrated in Fig. 2a. Changes in composition and microstructure may be observed from one laser track to another, and sometimes also inside one track. Part of the surface alloy (region A in Fig. 2b, corresponding to track n) displays the same hypoeutectic structure as the previous sample, consisting of dendrites of austenite with M_7C_3 carbides in the interdendritic areas. The related microhardness is about 500H_V. Local enrichment in

TABLE II Laser processing parameters selected

Sample number	Pre-coated powder	Surface coverage (mg cm^{-2})	Laser power (W)	Specific power (W mm^{-2})	Scanning speed (mm s^{-1})	Interaction time (s)	Shift %
1a	SiC	5.5	200	282	10	0.1	30
1b	SiC	6.5	200	282	10	0.1	30
1c	SiC	11.0	250	353	10	0.1	30
2a	C	2.0	200	282	5	0.2	30
2b	C	5.0	200	282	5	0.2	30
3	TiC	15.0	250	353	10	0.1	40
4	Ti + SiC	7.5	200	282	5	0.2	30

carbon may lead to a eutectic (γ–M_7C_3) structure (region B in Fig. 2b, belonging to track [$n + 1$]).

Large areas of a hard phase (about 1000 H_V) were also formed during the treatment. EPMA analysis carried out on a cross-section revealed that this phase contains a regular distribution of silicon (5.5 wt %), carbon (2.0 wt %), chromium (16 wt %), nickel (12 wt %), molybdenum (2 wt %) and manganese (1.5 wt %), the balance being iron. Cracks were frequently observed in those hard areas.

3.1.1.3. Surface coverage: 11 mg cm^{-2} (sample 1c). When increasing the amount of SiC incorporated in the melted pool, only the hard phase (about 1000 H_V) is present in the alloyed region. As shown for the previous sample, this layer is brittle and many cracks are observed (Fig. 3).

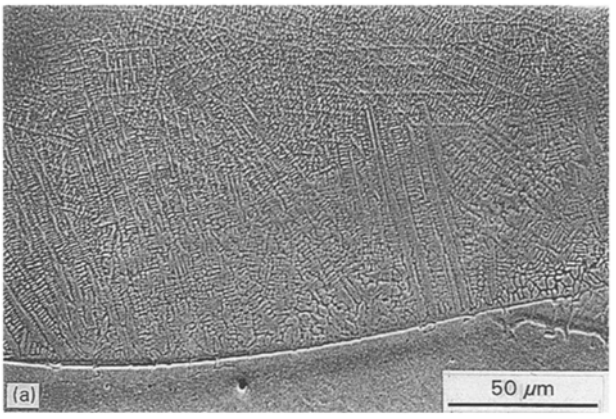

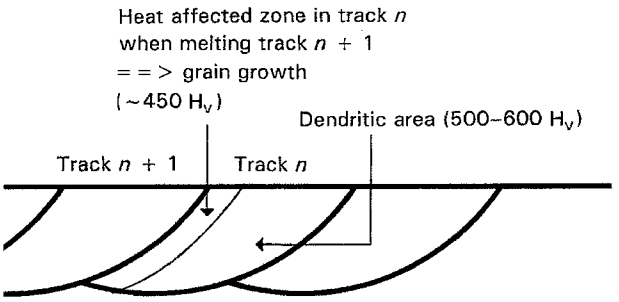

(b)

Figure 1 Sample 1a (316L–SiC): s.c. = 5.5 mg cm^{-2}, P = 200 W, v = 10 mm s^{-1}. (a) Secondary electron image showing the dendritic microstructure. (b) Schematic view of a transverse cross-section of the surface alloy.

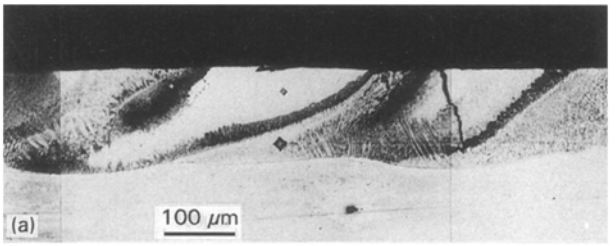

Figure 2 Sample 1b (316L–SiC): s.c. = 6.5 mg cm^{-2}, P = 200 W, v = 10 mm s^{-1}. (a) Optical micrograph of a transverse cross-section. (b) Backscattered electron image of the metallurgical structures and corresponding schematic view.

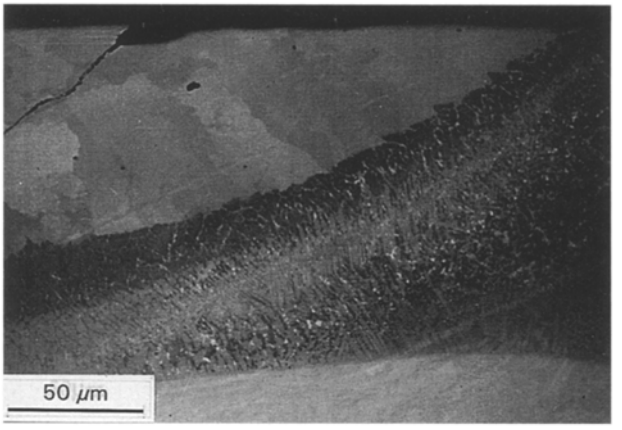

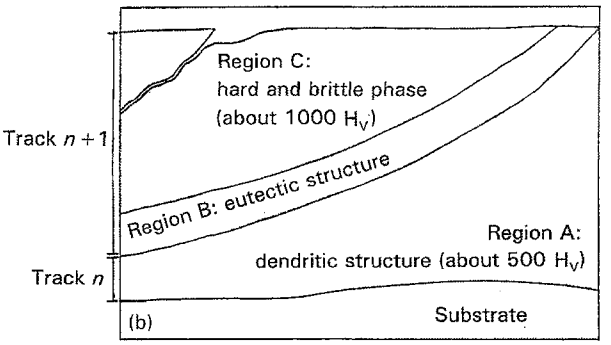

Figure 2 continued.

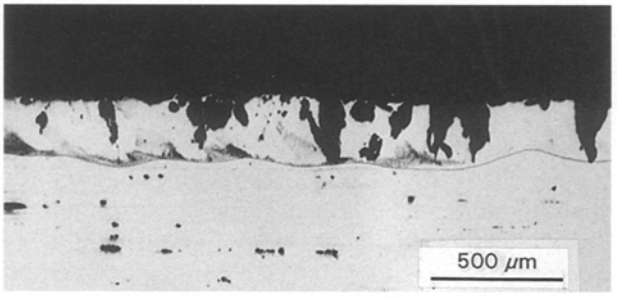

Figure 3 Optical micrograph of a transverse cross-section of sample 1c (316L–SiC, s.c. = 11 mg cm^{-2}, P = 250 W, v = 10 mm s^{-1}).

3.1.2. Carbon alloying

In order to complete our understanding on the role of the carbon in the hardening of 316L stainless steel, we focused our attention on the incorporation of carbon alone. As in previous experiments concerning SiC alloying, we have tested two surface coverages to obtain basic information on the structural changes and surface hardening.

3.1.2.1. Surface coverage: 2.0 mg cm^{-2} (sample 2a). XRD analysis showed the presence within the surface alloy of both austenite and M_7C_3 carbides. Fig. 4a shows the microstructure of the alloyed layer (about 120 μm). Fine dendrites of austenite are observed; the interdendritic area is composed of a eutectic austenite–M_7C_3 carbide (Fig. 4b). As previously mentioned for SiC alloying, the heat-affected zone of the tracks exhibits an increase in the size of the austenite

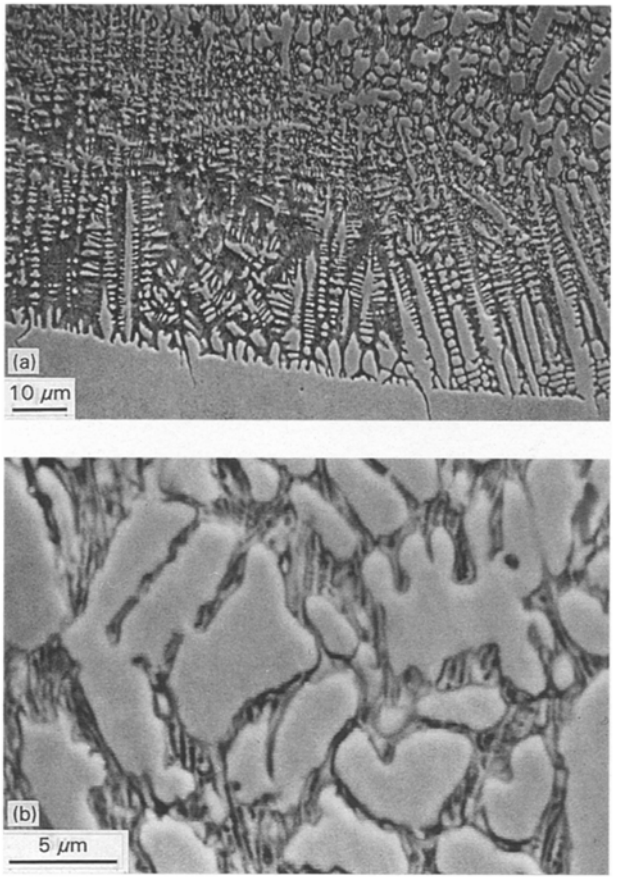

Figure 4 Sample 2a (316L–C): s.c. = 2 mg cm^{-2}, P = 200 W, v = 5 mm s^{-1}. (a) Secondary electron image showing the dendritic microstructure. (b) Secondary electron image showing the eutectic in the interdendritic areas.

cells or dendrites. EPMA showed that the concentration of carbon is nearly the same (about 1.2 wt %) all over the melted layer, which evidences the efficiency of the convectional flow of the liquid during melting. This alloy exhibits a hardness of about 420 H_V.

3.1.2.2. Surface coverage: 5.0 mg cm^{-2} (sample 2b). XRD analysis revealed the presence of austenite (γ) and carbides M_7C_3 (M = Cr, Fe). Fig. 5 shows the microstructure of the alloyed layer. The periphery of the tracks exhibits a dendritic (γ) microstructure leading to an averaged microhardness of 400 H_V, whereas the top centre of the tracks exhibits a eutectic (γ-M_7C_3) structure displaying a higher microhardness (650 H_V). The concentration of carbon in the eutectic area, measured by EPMA is about 3.0 wt %. The microstructural observations and hardness measurements are in good agreement; this means that hardness is the highest in the carbon richest areas. A thin layer (about 3 μm), resulting from a planar solidification is observed in the alloyed layer, at the interface with the unaffected substrate, where the solidification rate is minimum. We can notice that the surface alloy is crack-free even in the hardest areas.

The hypoeutectic and eutectic structures of the alloys obtained in this study are similar to those elaborated by Marsden *et al.* [12] on 420 stainless steel. In the present study, it could be thought that increasing further the carbon concentration would lead to the formation of hypereutectic alloys, but then, the problem of cracking, mentioned by Marsden *et al.* [12] for hypereutectic structures is likely to occur.

Figure 5 Secondary electron image of sample 2b (316L–C) showing the dendritic and eutectic structures (s.c. = 5 mg cm^{-2}, P = 200 W, v = 5 mm s^{-1}).

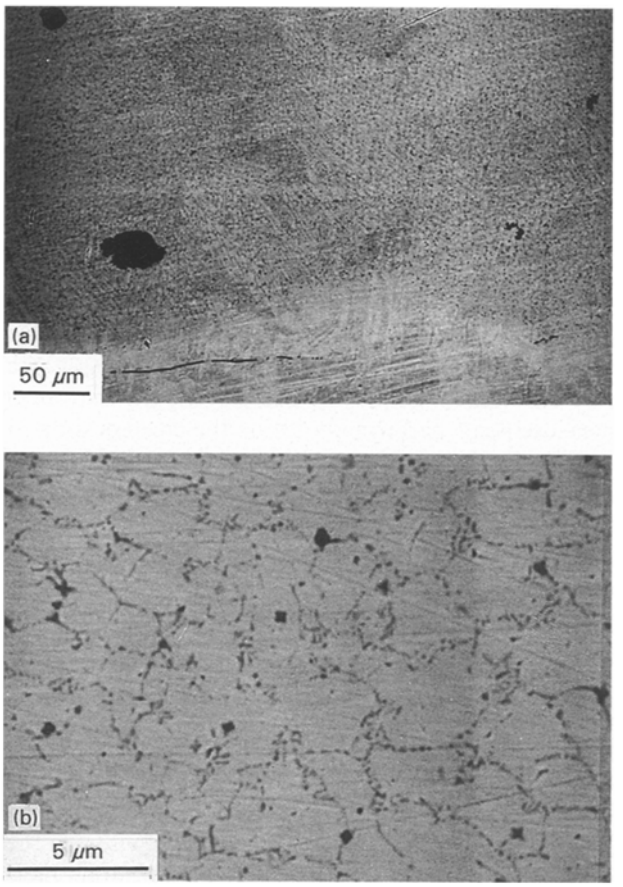

Figure 6 Sample 3 (316L–submicronic TiC) : s.c. = 15 mg cm^{-2} (5 treatments with 3 mg cm^{-2} each), P = 250 W, v = 10 mm s^{-1}. (a) Backscattered electron image of a transverse cross-section. (b) Backscattered electron image showing the microstructure outside the aggregates.

3.2. Hardening by titanium carbides

3.2.1. Incorporation of TiC submicronic particles (sample 3)

X-ray diffraction analysis showed the presence of TiC and austenite (γ) within the alloyed layer using the processing conditions described in Table II. A micrograph of a transversal cross-section of the alloy is illustrated in Fig. 6a. The alloyed layer appears to be

crack-free. Some large clusters of TiC, from 10 to 50 μm in size are distributed within the alloy. Outside these areas, the alloyed layer exhibits a regular microstructure (Fig. 6b) : the matrix is composed of austenite grains (dendrites) with TiC located in the interdendritic spacings. Some faceted crystals of TiC, about 1 μm in size, are also present, regularly distributed within the alloyed layer.

This overall microstructure is thought to result from the dissolution of the initial particles of TiC and their further precipitation during the solidification process. We had already observed a similar phenomenon for martensitic steels where the interdendritic precipitation of the αFe–TiC eutectic occurs [15]. In the present case, the main difference is that the matrix remains austenitic.

The dissolution of TiC particles is easy owing to their very small size: approximately 50 nm. This dissolution was also observed by Ayers and Tucker [9] who studied the hardening of 304 stainless steel by TiC but as a minor effect, because of the large size (100–200 μm) of the TiC particles used for their experiments. The large TiC clusters (10–50 μm) are thought to result from an agglomeration of powders to a size too large to allow their dissolution in the melt during the treatment. A similar phenomenon was also observed in the Fe–TiN system [16].

EPMA analyses have shown that about 70% of the incorporated TiC is located in these large clusters; this leads to a small concentration of TiC outside the clusters, about 3.5 wt %. Therefore, microhardness measurements performed outside the clusters showed only a slight increase in hardness (280 compared to 200 H_V for the substrate). In the experimental range investigated, we have never obtained greater hardening while keeping the alloyed coating homogeneous and avoiding cracks.

3.2.2. Ti + SiC coating (sample 4)

Laser alloying of 316L staniless steel with a mixture of titanium and SiC was planned because, on the one hand, laser alloying with submicronic TiC particles had lead to the formation of TiC aggregates irregularly dispersed in the resulting surface alloy while on the other hand, when using SiC, our observations have shown that SiC was totally dissociated into Si and C during laser melting. Therefore, laser melting of a Ti + SiC coating appeared as an interesting route to obtain a surface alloy enriched in silicon for corrosion applications [3], and strengthened by hard TiC precipitates resulting from the carburization of Ti.

The proportions of titanium and SiC in the coating were chosen so that the quantity of titanium in the melted pool is high enough to react with all the carbon brought by SiC and by the polymer (binding element).

The different phases detected by XRD are austenite (γ) , TiC and ferrite (α). The formation of ferrite is the result of the presence of silicon which is a ferrite former. Observation of the surface alloy showed a regular layer, about 130 μm thick (Fig. 7a). A regular dispersion of fine TiC precipitates, about 0.5 to 1 μm in diameter, was evidenced by SEM (Fig. 7b).

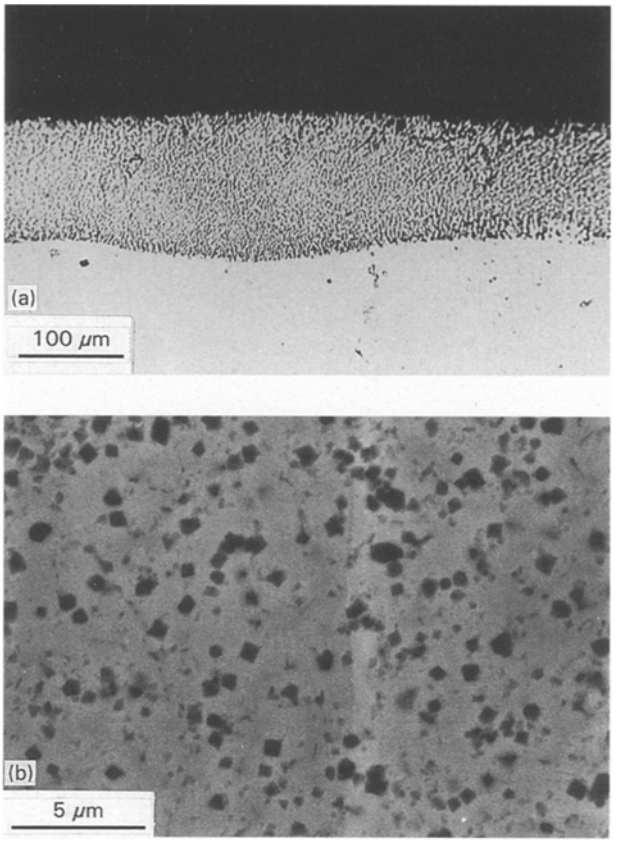

Figure 7 Sample 4 (316L–Ti + SiC): s.c. = 7.5 mg cm^{-2}, P = 200 W, v = 5 mm s^{-1}. (a) Optical micrograph of a transverse cross-section. (b) Backscattered electron image.

The concentration of TiC in this alloy, measured using EPMA is about 8 wt %. The average microhardness of the surface alloy is about 350 H_V but some areas within the alloy exhibit higher hardness (between 500 and 700 H_V); these areas must be TiC rich areas or (and) ferrite-rich areas.

The mixture (Ti + SiC) allowed to obtain a much more regular distribution of TiC (disappearance of TiC aggregates) within the surface alloy than submicronic TiC particles. Using this mixture as precursor, we made an alloyed layer containing about 8 wt % TiC with hardness values as high as 700 H_V and without any cracks.

4. Conclusions

Surface hardening of the 316L stainless steel was achieved by laser alloying with precursors leading to the precipitation of hard carbides during the solidification. For hardnesses lower than 900 H_V the alloyed layers were crack-free.

Alloying with SiC powders led to M_7C_3 carbide precipitation. This is the result of the dissociation of the silicon carbide during the laser irradiation. Surface alloys displaying homogeneous composition and microstructure and exhibiting a microhardness of 500–600 H_V were produced. Attempts to increase further the amounts of silicon and carbon in the surface layer led to the formation of a much harder (1000 H_V) but brittle coating.

Surface alloys produced by the incorporation of carbon alone contained austenite and M_7C_3 carbides.

Depending on the amount of carbon introduced, hypoeutectic and eutectic structures were obtained leading to typical microhardnesses of respectively 400 H_V and 650 H_V.

Hardening by titanium carbide precipitation was investigated using two precursors: submicronic TiC particles or a mixture of Ti and SiC powders. Only the second case allowed us to produce alloys exhibiting regular structure and composition with a noticeable hardness increase (between 350 and 700 H_V).

We plan now to test the tribological properties and the hot corrosion resistance of such surface alloys developed on the 316L stainless steel.

References

1. M. OHRING, "The materials science of thin films" (Academic Press, London, 1992).
2. P.A. MOLIAN, in "Surface modification technologies", edited by T.S. Sudarshan (Marcel Dekker, Inc., New York, 1989) p. 421.
3. A.Y. FASASI, S.K. ROY, M. PONS, A. GALERIE, D. SIBUET and M. CAILLET, in MAT-TEC 92, edited by A. Niku-Lari, (IITT International, Gournay/Marne, France, 1992) p. 211.
4. F. FOUQUET, J.M. PELLETIER, M. PILLOZ and A.B. VANNES, in "Laser de puissance et traitements des matériaux", edited by A.B. Vannes (Presses Polytechniques et Universitaires, Lausanne, Switzerland, 1991) p. 217.
5. M.C. SAHOUR, A.B. VANNES and J.M. PELLETIER, *J. Phys. IV, C7* **1** (1991) 51.
6. C.L. SEYTON, W.M. STEEN, K.G. WATKINS, M.G.S. FERREIRA, R.G.M. VILAR and P. CARVALHO, in MAT-TEC 92, edited by A. Niku-Lari (IITT International, Gournay/Marne, France, 1992) p. 219.
7. W.A. GLAESER, "Materials for tribology" (Elsevier, Amsterdam, 1992).
8. J.C. BAVAY in "Les aciers inoxydables", edited by P. Lacombe, B. Baroux and G. Beranger (Les Editions de Physique, Les Ulis, France, 1990) p. 567.
9. J.D. AYERS and T.R. TUCKER, *Thin Solid Films* **73** (1980) 201.
10. T.H. KIM and B.C. KIM, *J. Mater. Sci.* **27** (1992) 2967.
11. A. B. LYSENKO, N.N. KOZINA, T.V. GULYAEVA, V.V. SHIBAEV, A.G. GLUSHKOV, *Metallovedenie i Termicheskaya Obrabotka Metallov* **3** (1991) 2.
12. C. MARSDEN, D.R.F. WEST and W.M. STEEN, in "Laser surface treatment of metals", edited by C.W. Draper and P. Mazzoldi, NATO ASI Series E, no 115, (Martinus Nijhoff Publishers, Boston, 1986) p. 461.
13. C. RIEKER, D.G. MORRIS and J. STEFFEN, *Mat. Sci. Technol.* **5** (1989) 590.
14. M. TOMIE, N. ABE, S. NOGUCHI, Y. KITAHARA and Y. SATO, *Trans. JWRI* **20** (1991) 43.
15. C. TASSIN, M. PONS, A. Y. FASASI, A. GALERIE, G. SAINFORT and C. POLAK, *J. Mater. Sci.* in press.
16. T.H. KIM and B.G. SEONG, *ibid.* **25** (1990) 3583.

Received 2 February 1994
and accepted 20 January 1995